

SETUP AND COMMISSIONING OF THE DIAGNOSTICS BEAMLIN FOR THE SRF PHOTOINJECTOR PROJECT AT ROSSENDORF

T. Kamps*, D. Böhlick, M. Dirsat, D. Lipka, T. Quast, J. Rudolph, M. Schenk,
BESSY, Berlin, Germany

A. Arnold, F. Staufenbiel, J. Teichert, Forschungszentrum Dresden, Dresden, Germany
G. Klemz, I. Will, Max Born Institut, Berlin, Germany

Abstract

A superconducting radio frequency photo electron injector (SRF injector) has been developed by a collaboration of BESSY, DESY, FZD and MBI and is in operation since late 2007. After the initial commissioning in late 2007 with a Copper photocathode a Caesium-Telluride cathode was installed early 2008 to allow for high charge production. The longitudinal and transverse electron beam parameters are measured in a compact diagnostics beamline. This paper describes results from beam commissioning of the main diagnostic tools. Special emphasis is given on the bunch length measurement system for the 15 ps FWHM electron bunches. The system is based on the conversion of the electron pulses into radiation pulses by Cherenkov radiation. These radiation pulses are transported in a novel fully-reflective, relay imaging optical beamline to a streak camera, where the temporal properties of the pulses are measured.

EXPERIMENTAL SETUP

The setup for the SRF photoinjector consists of the SRF gun and a diagnostics beamline as depicted in Fig. 1. For more details on the SRF gun cavity and operational results see [1, 2]. The two operation modes of the SRF photoinjector are summarized in Tab.1. During the commission-

	ELBE FEL	High Charge
RF frequency		1.3 GHz
Beam energy		9.5 MeV
Operation		CW
Drive laser		263 nm
Photocathode		Cs ₂ Te
Pulse length FWHM	5 ps	16 ps
Repetition rate	13 MHz	500 kHz
Bunch charge	77 pC	1 nC
Trans. emittance	1.5 μ m	2.5 μ m

Table 1: Design beam parameters of the two main operation modes of the SRF injector: for the ELBE FEL replacing the thermionic gun (ELBE FEL) and at high bunch charge (High Charge).

ing of the SRF cavity, the gun was operated with a copper cathode, which has a quantum efficiency three orders of

*kamps@bessy.de

magnitude lower than Cs₂Te. The motivation for this is to separate the different commissioning stages and be able to fully test one subsystem after the other. The axis peak field of the accelerating mode is $E_{peak} = 50$ MV/m (design value). The current cavity is able to produce an accelerating field of $E_{acc} = 6$ MV/m, due to problems encountered during the cleaning process of the cavity [1].

BEAM CHARACTERIZATION

In order to characterize the performance of the photoinjector, the following beam parameters need to be considered:

- The energy distribution of the beam – the kinetic energy of the electrons and the energy spread. The beam momentum will vary between a few and 9.5 MeV. The minimum momentum spread as expected from simulations will be 36 keV for the low charge operation mode. These quantities will be measured in a 180 degree dipole spectrometer.
- The total beam intensity, together with the time structure. The bunch charge can vary between a few pC during initial operation with the Copper cathode and 1 nC at the high charge operation mode. The bunch charge is monitored with integrating current transformers and Faraday cups, the bunch length is measured with a Cherenkov monitor.
- The optical properties, which can be described in terms of the transverse beam emittance. The normalized beam emittance is expected to vary between 1 and 10 mm mrad. The electron beam generated in the injector is in all nominal operation modes space-charge dominated. For this reason a double slit-based phase space sampling method is considered, where an actuator-mounted slit mask is moved perpendicular across the beam.

For a complete description of the individual elements see [3]. In the following the tools to measure the transverse and temporal profile are described with more details. Furthermore initial experience gathered during commissioning is given.

TRANSVERSE PROFILE

Thin Yttrium-Aluminum-Garnet (YAG) crystal sheets doped with the visible light scintillator Cerium can be in-

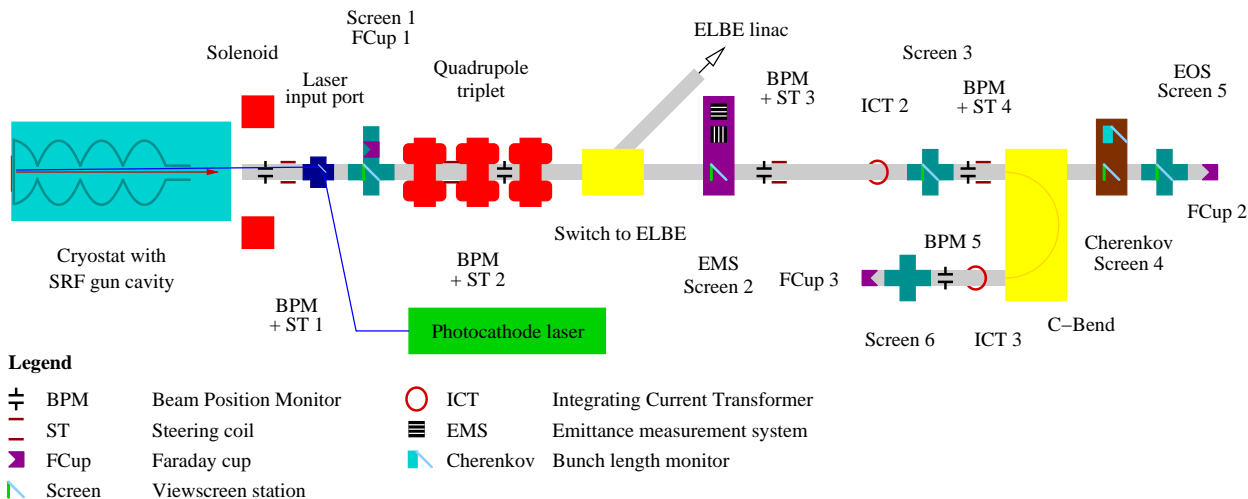


Figure 1: General setup of the SRF gun and diagnostics beamline.

serted into the beam path to produce an image of the transverse charge distribution. This beam image is detected by a CCD camera. The screen material has to be robust and UHV-compatible as the first screen is located in close proximity to the SRF cavity. To provide for the best image fidelity, the screens are mounted at normal incidence to the electron beam. An Aluminum mirror is placed downstream to deflect the fluorescent light out to the camera. Outside the vacuum beam pipe the light is deflected again by a mirror and then focused onto the sensitive area of a CCD camera. The optical focus and magnification can be calibrated by inserting a calibration target at the location of the screen. The cameras are GigE compliant, data transfer is done through standard ethernet cable in a dedicated camera network. The trigger for image acquisition is derived from the ELBE timing system. Standard photographic objective lenses with a focal length of 150 mm are used to image the screen image onto the sensitive area of the CCD camera. The minimum object size generated by the crystal screen is dominated by multiple scattering for beam energies below 10 MeV. At 2 to 3 MeV beam momentum the minimum resolution is around 40 μm and at 9.5 MeV the resolution is around 10 μm .

During commissioning, the viewscreens were able to withstand operation conditions with several thousand nC per hour without any visible degradation of the beam image. Fig. 2 shows a beam images obtained during commissioning.

TEMPORAL PROFILE

Cherenkov Monitor

The first temporal profile monitor is located after the spectrometer magnet in straight direction. Inside the Cherenkov monitor [4] the electron bunches pass a thin sheet of radiator. The radiator emits a Cherenkov radiation pulse with the same time structure as the electron

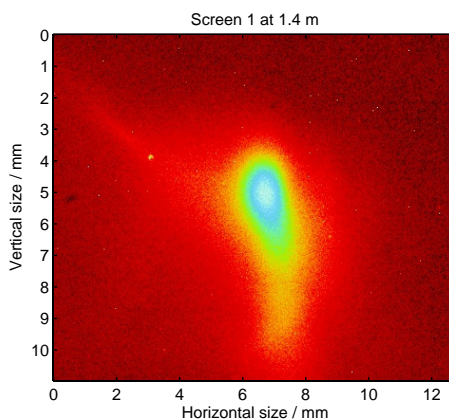


Figure 2: First beam image obtained with electrons from the Cs₂Te cathode.

bunch. A streak camera can be used to measure the shape and length of this radiation pulse with ps resolution. Silica aerogel plates of small dimensions with refractive index of $n = 1.008$ and 1.028 are available [5] and considered as Cherenkov radiator. The threshold energy for $n = 1.008$ is 4.1 MeV, for $n = 1.028$ is 2.2 MeV. The refractive index of the material was measured with samples in parallel plate setup. A test plate of thickness d was put perpendicular into the light path of a laser beam. The plate was rotated and the resulting parallel shift of the laser beam measured. From the measured parallel shift versus rotation angle data the refractive index could be retrieved. The thickness of the plate was chosen to be 6 mm to balance the amount of emitted photons with the time resolution due to dispersion. The Cherenkov light is then transported with mirrors to the streak camera [8] over a distance of roughly 20 m. The Cherenkov light exits the radiator with large divergence, therefore a relay imaging with focusing elements is necessary to achieve a high photon collection efficiency. Using lenses for this can cause dispersion related pulse broaden-

ing of the short photon pulse. For setups with lenses pulse broadening by a factor of 2.5 was measured for bunches of 20 ps FWHM length [6]. Therefore only reflective optical elements, plane and off-axis parabolic mirrors, were considered for the light transport. The pulse is broadened due to dispersion in the light beamline by 2.2 ps for wavelengths between 300 and 600 nm, caused to almost equal parts by the two viewports and the air in the light beamline. These effects can be minimized by using bandpass filters.

Laser Pulse Measurements

First tests with the streak camera were performed to check the photocathode laser (see [7] for full description) pulse length and the synchronisation of the streak camera to the master oscillator. For the direct measurement an optical transport line with mirrors and beamsplitters was setup to transport the laser light from the laser hutch to the neighboring streak camera hutch. Synchronization between laser and streak camera is achieved by a 250 MHz phase-locked loop synthesizer driven by a 13 MHz reference signal from the laser itself. The synchronization accuracy between laser and streak camera was measured to be better than 2 ps. The photocathode laser oscillator deliv-

ers pulses in the infra-red (1053 nm), which are amplified and finally in converted in two second harmonic generators to green (526nm) and finally ultra-violet (263 nm). During the data taking, the pump current of the photo diodes of the laser amplifier was changed and the average power and pulse length of the output pulses was measured. For measurement of the green pulses, the second conversion stage was removed. The average laser power was measured with a powermeter, the pulse length with the streak camera as described above. For each pump current setting, the light intensity was entering the streak camera was regulated, for the green pulses by low-reflectivity optical flats and neutral density filters, for the UV only with low-reflectivity flats. In Fig. 3 the results for these measurements are shown. For each data point five streak images were taken. Each image was analyzed by applying a Gaussian fit to the time-projection axis data. For the green pulses the average output power increases with increasing pump current. Above a pump current of 15.5 mA a sudden drop in laser intensity was observed. The laser intensity recovered soon, but due to time constraints the data point for this pump current could not be taken again. For the UV output pulses, the sequence started at high pump current. Here also the laser intensity dropped, this time at the data point for a pump current below 18.5 mA. The intensity for the measurement on the streak camera was consequently very low leading to a small signal to noise ratio and thus to an underestimation of the pulse length. It is planned to do the measurements again. The pulse length of the electron bunches after extraction out of the cathode as measured with a phase scan is $\Delta z = 18.1 \pm 7.3$ ps FWHM.

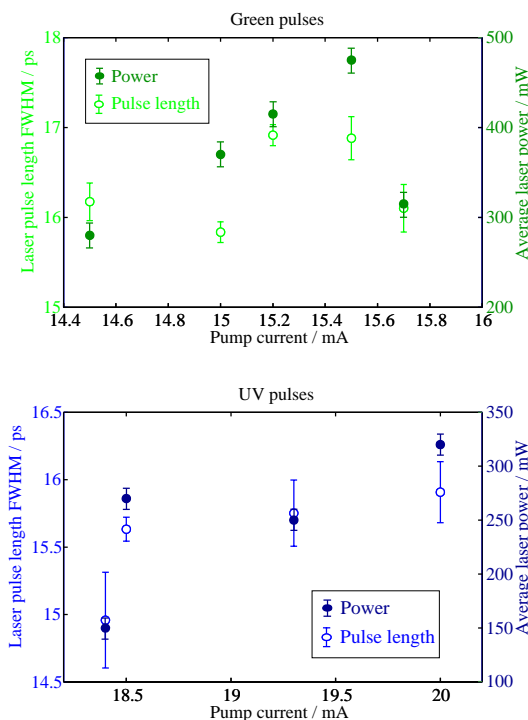


Figure 3: Results from laser pulse length measurements for the green (green and open points) and UV (blue and filled points) output of the laser for different pump currents.

ers pulses in the infra-read (1053 nm), which are amplified and finally in converted in two second harmonic generators to green (526nm) and finally ultra-violet (263 nm). During the data taking, the pump current of the photo diodes of the laser amplifier was changed and the average power and

SUMMARY AND OUTLOOK

The diagnostics beamline currently under construction plays a vital role in the commissioning and successful running of the SRF injector. Results from first beam tests at low bunch charge indicate the efficiency of the individual devices.

ACKNOWLEDGMENTS

We want to thank the engineers and technicians from BESSY, FZD and the Max Born Institute who contributed to the SRF injector project. We are grateful by the assistance received by DESY Hamburg and SLAC. We acknowledge the support by the German Federal Ministry of Education and Research Grant 05 ES4BR1/8.

REFERENCES

- [1] A. Arnold *et al.*, NIM A **577** (2007) 440-454.
- [2] J. Teichert *et al.*, WEPP105, these proceedings.
- [3] T. Kamps *et al.*, Proc. of BIW 2008, Lake Tahoe, 2008.
- [4] M. E. Conde *et al.*, PRST-AB **1** (1998) 041302.
- [5] A. Y. Barnyakov *et al.*, NIM A **553** (2005) 125-129.
- [6] D. Lipka, thesis, Humboldt University, Berlin, 2004.
- [7] I. Will *et al.*, Proc. of FEL 2006, Berlin, 2006.
- [8] Hamamatsu Photonics, 2003.